

See discussions, stats, and author profiles for this publication at: <https://www.researchgate.net/publication/51859410>

# Recognition of Hg<sup>2+</sup> and Cr<sup>3+</sup> in Physiological Conditions by a Rhodamine Derivative and Its Application as a Reagent for Cell-Imaging Studies

ARTICLE *in* INORGANIC CHEMISTRY · DECEMBER 2011

Impact Factor: 4.76 · DOI: 10.1021/ic2017243 · Source: PubMed

CITATIONS

79

READS

84

8 AUTHORS, INCLUDING:



**Sukdeb Saha**

Ben-Gurion University of the Negev

20 PUBLICATIONS 669 CITATIONS

SEE PROFILE



**Prasenjit Mahato**

Central Salt and Marine Chemicals Research I...

19 PUBLICATIONS 579 CITATIONS

SEE PROFILE



**Suresh Eringathodi**

Central Salt and Marine Chemicals Research I...

321 PUBLICATIONS 6,082 CITATIONS

SEE PROFILE



**Amitava Das**

CSIR - National Chemical Laboratory, Pune

195 PUBLICATIONS 4,745 CITATIONS

SEE PROFILE

# Recognition of $\text{Hg}^{2+}$ and $\text{Cr}^{3+}$ in Physiological Conditions by a Rhodamine Derivative and Its Application as a Reagent for Cell-Imaging Studies

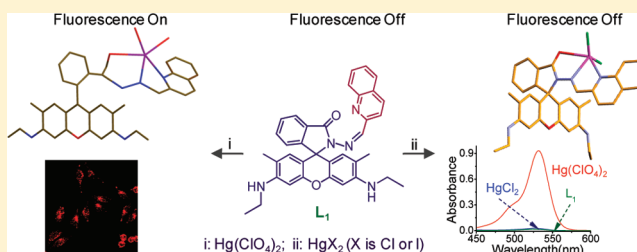
Sukdeb Saha,<sup>†</sup> Prasenjit Mahato,<sup>†</sup> Upendar Reddy G,<sup>†</sup> E. Suresh,<sup>†</sup> Arindam Chakrabarty,<sup>‡</sup> Mithu Baidya,<sup>‡</sup> Sudip K. Ghosh,<sup>\*,‡</sup> and Amitava Das<sup>\*,†</sup>

<sup>†</sup>Central Salt and Marine Chemicals Research Institute (CSIR), Bhavnagar 364002, Gujarat, India

<sup>‡</sup>Department of Biotechnology, Indian Institute of Technology, Kharagpur, West Bengal 721302, India

## S Supporting Information

**ABSTRACT:** A new rhodamine-based receptor, derivatized with an additional fluorophore (quinoline), was synthesized for selective recognition of  $\text{Hg}^{2+}$  and  $\text{Cr}^{3+}$  in an acetonitrile/HEPES buffer medium of pH 7.3. This reagent could be used as a dual probe and allowed detection of these two ions by monitoring changes in absorption and the fluorescence spectral pattern. In both instances, the extent of the changes was significant enough to allow visual detection. More importantly, the receptor molecule could be used as an imaging reagent for detection of  $\text{Hg}^{2+}$  and  $\text{Cr}^{3+}$  uptake in live human cancer cells (MCF7) using laser confocal microscopic studies. Unlike  $\text{Hg}(\text{ClO}_4)_2$  or  $\text{Hg}(\text{NO}_3)_2$  salts,  $\text{HgCl}_2$  or  $\text{HgI}_2$  failed to induce any visually detectable change in color or fluorescence upon interaction with  $\text{L}_1$  under identical experimental conditions. Presumably, the higher covalent nature of  $\text{Hg}^{\text{II}}$  in  $\text{HgCl}_2$  or  $\text{HgI}_2$  accounts for its lower acidity and its inability to open up the spirolactam ring of the reagent  $\text{L}_1$ . The issue has been addressed on the basis of the single-crystal X-ray structures of  $\text{L}_1 \cdot \text{HgX}_2$  ( $\text{X}^- = \text{Cl}^-$  or  $\text{I}^-$ ) and results from other spectral studies.



## INTRODUCTION

The design of optical sensors for selective recognition and sensing of desired metal ions is an important and contemporary research area. In this regard, metal ions that are known to have detrimental effects on living organisms or the environment are generally more common as target metal ions for such studies.<sup>1</sup> Apart from this, other critical aspects like signal transduction and the possibility of using these reagents in physiological conditions generally influence the receptor design.<sup>2</sup> The  $\text{Hg}^{2+}$  ion is considered to be one of the most toxic metal ions and thus one of the most common among different metal ions that are being studied for recognition studies. The extreme toxicity of mercury and its derivatives results from their affinities toward thiol groups in proteins and enzymes.<sup>3</sup> This leads to the malfunctioning of the living cells and eventually leads to serious health hazards. More importantly, the  $\text{Hg}^{2+}$  ion present in soil or in effluent water is assimilated by the lower aquatic organisms, which are known to convert it to methylmercury, one of the most potent neurotoxins for human race.<sup>4</sup> Reports also reveal that this methylmercury moves upward in the food chain through the marine predator animals and bioaccumulates in human beings with manifestation of different neurological disorders.<sup>5</sup> Bioaccumulation of  $\text{Hg}^{2+}$  from atmospheric deposition is also known to happen in certain mosses and tree leaves, and this adversely affects photosynthesis and transpiration in plants; the former is believed to have an impact

on the global carbon cycle.<sup>6</sup> Unlike  $\text{Hg}^{2+}$ ,  $\text{Cr}^{3+}$  is less harmful to human life, though chromium present in other higher oxidation states (4+ and 6+) has a grave consequence on human health.  $\text{Cr}^{3+}$  is an effective nutrient and gives immunity power to the human body to prevent various diseases like diabetes, cardiovascular disease, etc.<sup>7</sup> Further, its deficiency is known to influence the metabolism of glucose and lipids adversely and causes maturity-onset diabetes, cardiovascular diseases, and nervous system disorders.<sup>8</sup> However, exposure to higher concentrations of  $\text{Cr}^{3+}$  is known to inflict a negative effect on normal enzymatic activities. A recent study reveals that soluble  $\text{Cr}^{3+}$  at pH 6–8 can be found transiently in significant concentrations and has an adverse influence on microorganisms, like *Shewanella* sp. MR-4.<sup>9</sup> The  $\text{Cr}^{3+}$  ion, present in the cytoplasm, is known to bind nonspecifically to DNA and other cellular components, and these processes become important when the concentration of  $\text{Cr}^{3+}$  exceeds a certain threshold value. These are known to inhibit DNA transcription and possibly replication.<sup>10</sup> All of these have made it almost obligatory to develop efficient sensor molecules, which can be used for the efficient and selective detection of these two ions present in trace quantities. These reagents may become even more versatile if these are found to work in an aqueous

Received: August 8, 2011

Published: December 12, 2011

environment and at physiological pH because this opens up the possibility for their *in vivo* application. Both of these metal ions are known to be extensively solvated in an aqueous medium, and the unfavorably high enthalpy of solvation poses a challenge to chemists in developing a suitable receptor for sensing of these ions in an aqueous environment; to date, methods for monitoring the actual concentration of  $\text{Hg}^{2+}$  or  $\text{Cr}^{3+}$  *in vivo* are rather limited.<sup>7c,8a,11</sup>

Current approaches for environmental and clinical samples rely on costly, time-consuming methods like atomic absorption/emission spectroscopy or inductively coupled plasma mass spectrometry,<sup>12</sup> which are not very convenient and handy for “in-field” detection. These limitations have actually set off an enormous interest among chemists for the development of efficient, cost-effective, and reversible chemosensors for  $\text{Hg}^{2+}$  and  $\text{Cr}^{3+}$ . Although a number of selective sensors for  $\text{Hg}^{2+}$  have been devised using various modes of signal transduction processes through detectable changes in either redox<sup>13</sup> or spectral (electronic and fluorescence)<sup>14,15</sup> properties, such examples are uncommon for  $\text{Cr}^{3+}$  in the literature. In this regard, a receptor molecule that could be used as a dual probe for the detection and sensing of the desired metal ions by probing the metal-ion binding induced changes in the electronic as well as fluorescence spectral properties because the output signal has a distinct edge over other receptors because these receptors could be used either as colorimetric or fluorogenic sensors. Colorimetric sensors allow easy in-field detection, while fluorescence-based sensors provide an edge in imaging studies.  $\text{Hg}^{2+}$  and  $\text{Cr}^{3+}$  are known to quench effectively the excited state of the fluorophore through an efficient spin-orbit coupling and paramagnetic effect, respectively.<sup>16</sup> Thus, examples of fluorescence-based reversible sensor molecules for these two ions for sensing and imaging applications are not common, except the reagents that were designed based on the spirolactam to open ring amide equilibrium process of rhodamine derivatives.<sup>17</sup> Appropriately functionalized rhodamine derivatives belong to a class of receptors that allow detection of  $\text{Hg}^{2+}$  present in an aqueous solution through visually detectable changes in color, as well as through a *switch-on* fluorescence response. This dual detection mode has made various rhodamine derivatives an attractive choice for the design of receptors for  $\text{Hg}^{2+}$ . However, examples for the use of rhodamine derivatives for the recognition of  $\text{Cr}^{3+}$  in the aqueous environment are limited.<sup>18</sup> In this article, we report a new rhodamine derivative that binds specifically to  $\text{Hg}^{2+}$  and  $\text{Cr}^{3+}$  in the presence of a large excess of other common alkali, alkaline earth, and all common transition-metal ions. All previous references on  $\text{Hg}^{2+}$  recognition using rhodamine derivatives describe the use of  $\text{Hg}(\text{NO}_3)_2$  or  $\text{Hg}(\text{ClO}_4)_2$  salts, which induce a spirolactam ring-opening reaction upon coordination to the  $\text{Hg}^{2+}$  ion with associated *switch-on* responses at  $\sim 530$  nm for the electronic spectra and at  $\sim 560$  nm for the fluorescence spectra.<sup>17</sup> These allow a visual detection, as well as usage as an imaging agent for the *in vitro* and *in vivo* detection of  $\text{Hg}^{2+}$  in physiological conditions.<sup>19</sup> However, literature reports on the use of  $\text{HgCl}_2$  for recognition studies are very limited. Two independent reports reveal that  $\text{HgCl}_2$  initiates an irreversible and stoichiometric reaction between adjacent thiourea and cyclic amide functionalities to yield an oxadiazole derivative with an associated spirolactam ring-opening reaction that leads to the generation of a strongly luminescent xanthene form.<sup>20</sup> The only other two references that described the use of  $\text{HgCl}_2$  for sensing studies reported the

use of the same thiospiro derivative of rhodamine B. On the basis of mass spectral evidence, it was proposed that, in both studies, the  $\text{Hg}^{2+}$  ion was initially coordinated to a thiocarboxylate derivative of the xanthene form of rhodamine B, which subsequently underwent a hydrolysis reaction to generate the corresponding carboxylate derivative.<sup>21</sup> In one of these four examples, a mechanistic pathway involving  $\text{HgCl}_2$  was proposed in an intermediate. However, X-ray structural evidence for such a proposition remained elusive. Literature reports reveal that  $\text{HgCl}_2$  and  $\text{HgI}_2$ , two commonly available halide salts, are more covalent in nature.  $\text{HgCl}_2$  possesses only 23% ionic character, while  $\text{HgI}_2$  has even less ionic character.<sup>22</sup> Interaction of such a nonionic  $\text{Hg}^{\text{II}}$  center with a spirolactam derivative is not well understood, and this is discussed in this manuscript with single-crystal structural evidence using a new reagent, **L**<sub>1</sub>. This new reagent, **L**<sub>1</sub>, could be used as a reversible and selective fluorogenic, as well as colorimetric sensor for  $\text{Hg}^{2+}$  and  $\text{Cr}^{3+}$  in a mixed aqueous medium [ $\text{CH}_3\text{CN}$ /aqueous HEPES buffer (1 mM; 3:2, v/v)] at a physiological pH (pH 7.3). We have also shown that this receptor could be used for detecting uptake of the  $\text{Hg}^{2+}$  ion by living cells from an aqueous solution containing  $\text{Hg}^{2+}$  at pH 7.3 through cell imaging studies. In the present study, we have incorporated a quinoline unit with the aim of having another fluorescent fragment, along with the Rhodamine 6G derivative, to enable us to probe the metal-ion recognition processes at two different monitoring wavelengths of the fluorescence spectrum to avoid the possibility of any interference at any particular wavelength. However, no quinoline-based fluorescence was observed for either free **L**<sub>1</sub> or **L**<sub>1</sub> bound to  $\text{Hg}^{2+}$  or  $\text{Cr}^{3+}$ . The reasons for such an observation are also discussed.

## ■ EXPERIMENTAL SECTION

Rhodamine 6G hydrochloride, quinoline-2-aldehyde,  $\text{LiClO}_4$ ,  $\text{NaClO}_4$ ,  $\text{KClO}_4$ ,  $\text{CsClO}_4$ ,  $\text{Mg}(\text{ClO}_4)_2$ ,  $\text{Ca}(\text{ClO}_4)_2$ ,  $\text{Ba}(\text{ClO}_4)_2$ ,  $\text{Sr}(\text{ClO}_4)_2$ ,  $\text{Cu}(\text{ClO}_4)_2$ ,  $\text{Zn}(\text{ClO}_4)_2$ ,  $\text{Co}(\text{ClO}_4)_2$ ,  $\text{Ni}(\text{ClO}_4)_2$ ,  $\text{Cr}(\text{ClO}_4)_3$ ,  $\text{Fe}(\text{ClO}_4)_2$ ,  $\text{Fe}(\text{ClO}_4)_3$ ,  $\text{Cd}(\text{ClO}_4)_2$ ,  $\text{Hg}(\text{ClO}_4)_2$ , and  $\text{Pb}(\text{ClO}_4)_2$  were obtained from Sigma-Aldrich and used as received. All of the other reagents used were procured from S. D. Fine Chemicals, India. Hydrazine hydrates, glacial acetic acid, acetonitrile, methanol (AR; Merck), and ethanol (Spectrosol; Spectrochem, India) were used as solvents. HPLC-grade water (Merck, India) was used for experiments and spectral studies. The Rhodamine 6G hydrazine derivative (**L**) was synthesized following the reported procedure.<sup>23</sup> Electrospray ionization mass spectrometry (ESI-MS) measurements were carried out on a Waters QToF-Micro instrument. Microanalysis (C, H, and N) was performed using a Perkin-Elmer 4100 elemental analyzer. Fourier transform infrared (FTIR) spectra were recorded as KBr pellets using a Perkin-Elmer Spectra GX 2000 spectrometer.  $^1\text{H}$  and  $^{13}\text{C}$  NMR spectra were recorded on a Bruker 500 MHz FT NMR (model Avance-DPX 500). Electronic spectra were recorded with a Shimadzu UV-3101 PC/Varian Cary 500 Scan UV-vis-near-IR spectrophotometer. Emission spectra were recorded using an Edinburgh Instruments model Xe-900. Time-resolved fluorescence measurements were carried out using a time-correlated single-photon-counting (TCSPC) technique using an Edinburgh Instruments model OB920. A 360 nm light-emitting diode (LED) was used as the excitation source for the present studies.

Crystals of suitable size were selected from the mother liquor, immersed in paratone oil, then mounted on the tip of a glass fiber, and cemented using epoxy resin. Intensity data for both crystals were collected using  $\text{Mo K}\alpha$  ( $\lambda = 0.71073$  Å) radiation on a Bruker SMART APEX diffractometer equipped with a CCD area detector at 110 K. The data integration and reduction were processed with SAINT software.<sup>24a</sup> An empirical absorption correction was applied to the collected reflections with SADABS.<sup>24b</sup> The structures were solved by

direct methods using *SHELXTL*<sup>24c</sup> and were refined on  $F^2$  by the full-matrix least-squares technique using the *SHELXL*-97 program.<sup>24d</sup> All non-hydrogen atoms were refined anisotropically until convergence was reached. Hydrogen atoms attached to the ligand moieties and solvents of crystallization were stereochemically fixed in both complexes. The diagrams of the crystal structures were generated using *Mercury* 2.3. A summary of the crystallographic data and details of data collection for all three compounds are given in Table 1.

**Table 1.** Crystallographic Data for  $L_1 \cdot [HgCl_2]$  and  $L_1 \cdot [HgI_2]$

identification code	$L_1 \cdot [HgCl_2]$	$L_1 \cdot [HgI_2]$
CCDC number	CCDC 832870	CCDC 832871
empirical formula	$C_{75}H_{72}Cl_{10}Hg_2N_{10}O_5$	$C_{36}H_{33}HgI_2N_5O_2$
fw	1949.11	1022.06
temperature (K)	110(2)	110(2)
wavelength (Å)	0.710 73	0.710 73
cryst syst	monoclinic	monoclinic
space group	$C2/c$	$C2/c$
<i>a</i> (Å)	32.831	38.4292(17)
<i>b</i> (Å)	17.1862(11)	9.4617(4)
<i>c</i> (Å)	29.3246(18)	19.7407(9)
$\beta$ (deg)	110.4270(10)	105.3580(10)
volume (Å <sup>3</sup> )	15505.8(17)	6921.5(5)
<i>Z</i>	8	8
density (calcd) (Mg m <sup>-3</sup> )	1.670	1.962
abs coeff (mm <sup>-1</sup> )	4.357	6.271
<i>F</i> (000)	7696	3888
crystal size (mm <sup>3</sup> )	0.64 × 0.43 × 0.38	0.35 × 0.14 × 0.11
reflections	45 481	20 208
independent	17 947 [ <i>R</i> (int) = 0.0297]	8038 [ <i>R</i> (int) = 0.0234]
refinement method	full-matrix least squares on $F^2$	full-matrix least squares on $F^2$
data/restraints/no. of parameters	17 947/0/945	8038/0/427
GOF on $F^2$	1.018	1.145
final <i>R</i> indices [ <i>I</i> > 2σ( <i>I</i> )]	<i>R</i> 1 = 0.0380, <i>wR</i> 2 = 0.0996	<i>R</i> 1 = 0.0289, <i>wR</i> 2 = 0.0813
<i>R</i> indices (all data)	<i>R</i> 1 = 0.0469, <i>wR</i> 2 = 0.1035	<i>R</i> 1 = 0.0340, <i>wR</i> 2 = 0.0991
largest diff peak and hole (e Å <sup>-3</sup> )	1.804 and -1.314	1.323 and -0.656

MCF7 cells were grown in Dulbecco's Modified Eagle Medium supplemented with 10% fetal bovine serum at 37 °C were trypsinized, and  $1 \times 10^4$  cells were added in each well in a 24-well culture plate. After 48 h of growth, the cells were treated with different concentrations (0–4.0 μM) of  $Cr(ClO_4)_3$  and  $Hg(ClO_4)_2$  dissolved in 1X phosphate-buffered saline for 1 h. MCF7 cells were then stained with a 4 μM solution of  $L_1$  dissolved in acetonitrile/aqueous HEPES (3:2, v/v) for 60 min at 37 °C. Cells were viewed under a laser scanning confocal microscope (FV100, Olympus) at an excitation wavelength of 543 nm.

**Synthesis of  $L_1$ .** Rhodamine 6G hydrazine ( $L_1$ ) (300 mg, 0.646 mmol) and quinoline-2-aldehyde (101 mg, 0.646 mmol) were dissolved in 20 mL of methanol. To this was added approximately 2 drops of acetic acid, and the resulting solution was refluxed for 10 h. An off-white precipitate was found. The reaction mixture was allowed to attain room temperature, and then the precipitate was collected through filtration. The residue was washed thoroughly with methanol to isolate  $L_1$  in pure form with 76% yield (the yield was calculated based on the starting reagents). <sup>1</sup>H NMR [500 MHz,  $CDCl_3$ ,  $SiMe_4$ , *J* (Hz), δ (ppm)]: 8.530 (1H, s,  $-CH_{10}=N-$ ), 8.117 (1H, d, *J* = 9, ArH<sub>7</sub>), 8.056–8.013 (1H, m, ArH<sub>14</sub>), 7.975 (1H, d, *J* = 9, ArH<sub>13</sub>), 7.719 (1H, d, *J* = 8, ArH<sub>16</sub>), 7.618 (1H, t, *J* = 8, ArH<sub>15</sub>), 7.513–7.443 (4H, m, ArH<sub>2</sub>, H<sub>3</sub>, H<sub>4</sub>, H<sub>5</sub>), 7.08 (1H, d, *J* = 7, ArH<sub>8</sub>), 6.453 (2H, s,

ArH<sub>20</sub>, H<sub>29</sub>), 6.382 (2H, s, ArH<sub>23</sub>, H<sub>26</sub>), 3.477 (2H, s,  $-NH-$ ), 3.21 (4H, q, H<sub>32</sub>, H<sub>34</sub>), 1.860 (6H, s, H<sub>31</sub>, H<sub>36</sub>), 1.306 (6H, t, H<sub>33</sub>, H<sub>35</sub>). <sup>13</sup>C NMR [125 MHz,  $CDCl_3$ ,  $SiMe_4$ , δ (ppm)]: 165.804, 155.049, 152.894, 151.458, 147.949, 147.815, 146.433, 135.965, 134.072, 129.525, 129.463, 128.492, 128.406, 128.075, 127.717, 127.544, 126.960, 123.902, 118.242, 106.206, 97.304, 66.209, 38.555, 16.885, 14.948. ESI-MS (positive mode, *m/z*). Calcd for  $C_{36}H_{33}N_5O_2$ : 567.58. Found: 568.34 (40%;  $M + H^+$ ), 590.33 (100%;  $M + Na^+$ ). Elem Anal. Calcd: C, 76.17; H, 5.86; N, 12.34; O, 5.64. Exptl: C, 75.8; H, 5.9; N, 12.3.

#### General Methodology Adopted for Spectroscopic Studies.

A solution of the perchlorate salts of the respective ions ( $Li^+$ ,  $K^+$ ,  $Na^+$ ,  $Ca^{2+}$ ,  $Mg^{2+}$ ,  $Fe^{2+}$ ,  $Fe^{3+}$ ,  $Co^{2+}$ ,  $Ni^{2+}$ ,  $Cu^{2+}$ ,  $Zn^{2+}$ ,  $Cd^{2+}$ ,  $Pb^{2+}$ ,  $Ba^{2+}$ ,  $Sr^{2+}$ ,  $Cr^{3+}$ , and  $Hg^{2+}$ ) was used for the studies. For checking the relative, but qualitative, binding affinity of individual metal ions toward the reagent  $L_1$ , the effective metal-ion concentration in acetonitrile/aqueous HEPES buffer (1 mM; 3:2, v/v) was maintained at  $1.0 \times 10^{-4}$  M, while that for the receptor  $L_1$  was maintained at  $7.0 \times 10^{-6}$  M. The solution pH was found to be 7.3.

**Evaluation of the Association Constant for the Formation of  $L_1 \cdot Hg^{2+}$  and  $L_1 \cdot Cr^{3+}$ .** Receptor  $L_1$  was dissolved in acetonitrile/aqueous HEPES buffer (1 mM; 3:2, v/v; pH 7.3) and stored in dark conditions. This solution composition was maintained for all spectrophotometric titration studies. A stock solution of  $Hg(ClO_4)_2$ , having a concentration of  $1.18 \times 10^{-3}$  M, was prepared in the same solvent composition. A solution of  $L_1$  having an effective concentration of  $7.05 \times 10^{-6}$  M was used for spectroscopic titrations, while final concentrations for the  $Hg^{2+}$  ion were varied between 0 and  $7.13 \times 10^{-4}$  M. All solutions were stored at 25 °C. The solution pH was adjusted to 7.3 using an aqueous HEPES buffer solution having an effective concentration of 1 mM.

An effective concentration of  $7.76 \times 10^{-6}$  M for  $L_1$  in acetonitrile/aqueous HEPES buffer (1 mM; 3:2, v/v; pH 7.3) was used for titration studies with a  $Cr^{3+}$  solution. A  $1.46 \times 10^{-3}$  M stock solution of  $Cr(ClO_4)_3$  was prepared in the same solvent composition and was used for spectrophotometric titration studies, while effective concentrations of  $Cr^{3+}$  were varied between 0 and  $1.02 \times 10^{-3}$  M. The solution pH was maintained at 7.3 using an aqueous HEPES buffer solution with an effective concentration of 1 mM.

#### General Methodology Adopted for Fluorescence Studies.

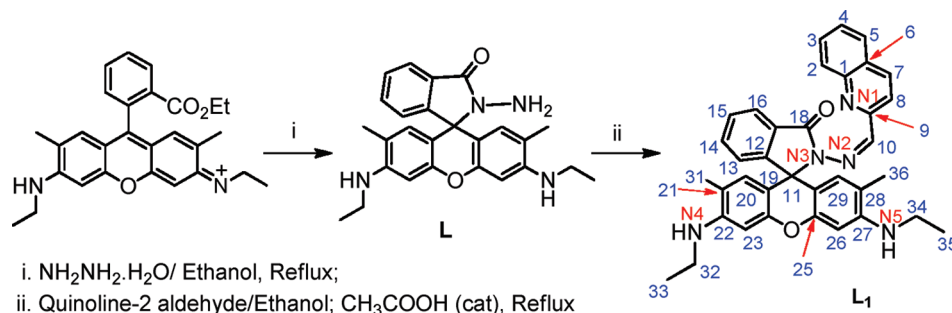
A solution of the perchlorate salts of the respective ions ( $Li^+$ ,  $Na^+$ ,  $K^+$ ,  $Ca^{2+}$ ,  $Mg^{2+}$ ,  $Ba^{2+}$ ,  $Sr^{2+}$ ,  $Fe^{2+}$ ,  $Fe^{3+}$ ,  $Co^{2+}$ ,  $Ni^{2+}$ ,  $Cu^{2+}$ ,  $Zn^{2+}$ ,  $Cd^{2+}$ ,  $Pb^{2+}$ ,  $Ba^{2+}$ ,  $Sr^{2+}$ ,  $Cr^{3+}$ , and  $Hg^{2+}$ ) in a spectroscopic-grade acetonitrile/aqueous HEPES buffer (1 mM; 3:2, v/v; pH 7.3) solvent mixture was used for the studies, while maintaining an effective concentration of the respective metal ion at  $2.0 \times 10^{-4}$  M. A solution of the receptor  $L_1$  with an effective concentration of  $10.0 \times 10^{-6}$  M was prepared in the same mixed-solvent medium and was used for checking the relative binding affinity with different metal ions.

**Evaluation of the Association Constant for the Formation of  $L_1 \cdot Hg^{2+}$  and  $L_1 \cdot Cr^{3+}$ .** Receptor  $L_1$  with an effective concentration of  $7.0 \times 10^{-6}$  M in an acetonitrile/aqueous HEPES buffer (1 mM; 3:2, v/v; pH 7.3) was used for the emission titration studies with a  $Hg^{2+}$  solution. A stock solution of  $Hg(ClO_4)_2$ , having a concentration of  $8.41 \times 10^{-3}$  M in an acetonitrile/aqueous HEPES buffer (3:2, v/v; pH 7.3) solution was used.

The formation constant for  $L_1 \cdot Cr^{3+}$  was also evaluated from fluorescence titration data. For this, the effective concentration of  $L_1$  was maintained at  $7.76 \times 10^{-6}$  M in acetonitrile/aqueous HEPES buffer (3:2, v/v; pH 7.3), while a stock solution of  $Cr^{3+}$  having a concentration of  $2.54 \times 10^{-3}$  M in an acetonitrile/aqueous HEPES buffer (3:2, v/v) medium of pH 7.3 was used for this study. The effective  $Cr^{3+}$  concentration was varied between 0 and  $7.93 \times 10^{-4}$  M for this titration. In both cases, the solution pH was adjusted to 7.3 using an aqueous HEPES buffer solution having an effective concentration of 1 mM.

**Calculations for the Binding Constants Using Spectrophotometric Titration Data.** The association constant and stoichiometry for the formation of the respective complexes were evaluated using the Benesi–Hildebrand (B–H) plot (eq 1).<sup>25</sup>



Scheme 1. Methodology Adopted for the Synthesis of  $L_1$ 

$$\frac{1}{(A - A_0)} = \frac{1}{K(A_{\text{max}} - A_0)[M^{n+}]} + \frac{1}{(A_{\text{max}} - A_0)} \quad (1)$$

$A_0$  is the absorbance of  $L_1$  at absorbance maxima ( $\lambda = 527$  nm for  $\text{Hg}^{2+}$  and  $531$  nm for  $\text{Cr}^{3+}$ ),  $A$  is the observed absorbance at that particular wavelength in the presence of a certain concentration of the metal ion ( $M^{n+}$ ),  $A_{\text{max}}$  is the maximum absorbance value that was obtained at  $\lambda = 527$  nm ( $\text{Hg}^{2+}$ ) or  $531$  nm ( $\text{Cr}^{3+}$ ) during titration with varying  $[M^{n+}]$ ,  $K$  is the association constant ( $\text{M}^{-1}$ ) and was determined from the slope of the linear plot, and  $[M^{n+}]$  is the concentration of the  $\text{Hg}^{2+}$  or  $\text{Cr}^{3+}$  ion added during titration studies. The goodness of the linear fit of the B–H plot of  $1/(A - A_0)$  vs  $1/[\text{Hg}^{2+}]$  or  $1/[\text{Cr}^{3+}]$  for 1:1 complex formation confirms the binding stoichiometry between  $L_1$  and  $\text{Hg}^{2+}$  or  $\text{Cr}^{3+}$ .

$$\frac{1}{(I - I_0)} = \frac{1}{K(I_{\text{max}} - I_0)[M^{n+}]} + \frac{1}{(I_{\text{max}} - I_0)} \quad (2)$$

Binding stoichiometries for the respective complex formations were also confirmed from Job's plot. In the case of evaluation of the binding constant from the results of fluorescence titration, a modified B–H equation (eq 2) was used, where  $I_0$ ,  $I_{\text{max}}$ , and  $I$  represent the emission intensity of free  $L_1$ , the maximum emission intensity observed in the presence of added metal ion at  $555$  nm for  $\text{Hg}^{2+}$  ( $\lambda_{\text{ext}} = 500$  nm) or  $557$  nm for  $\text{Cr}^{3+}$  ( $\lambda_{\text{ext}} = 500$  nm), and the emission intensity at a certain concentration of the metal ion added, respectively.

## RESULTS AND DISCUSSION

An intermediate spirolactam form of the rhodamine derivative ( $L$ ) was synthesized following a reported procedure by reacting (*E*)-ethyl-2-[6-(ethylamino)-3-(ethylimino)-3*H*-xanthen-9-yl]-benzoate with hydrazine hydrate.<sup>23</sup> The purity of this intermediate was checked by standard analytical and spectroscopic techniques (Supporting Information). Receptor  $L_1$  was synthesized following a Schiff base type reaction between the intermediate spirolactam derivative ( $L$ ) and quinoline-2-aldehyde in methanol as the solvent (Scheme 1). A small amount (2 or 3 drops) of  $\text{CH}_3\text{COOH}$  was added in the reaction medium as a catalyst. A white precipitate appeared and was isolated through filtration. This white residue was thoroughly washed with methanol and air-dried. The results of the various analytical and spectroscopic data (elemental analysis,  $^1\text{H}$  and  $^{13}\text{C}$  NMR, FTIR, and ESI-MS) confirmed the desired purity of the reagent  $L_1$ , and this was used further for recognition studies. This newly synthesized compound  $L_1$  was found to have a limited solubility in water, and thus an acetonitrile/aqueous HEPES buffer (3:2, v/v) solution was used for our studies. The solution of  $L_1$  in an acetonitrile/aqueous HEPES buffer (3:2, v/v) medium was colorless, which revealed that  $L_1$  was present almost exclusively in the spirolactam form under the experimental conditions. The  $^{13}\text{C}$  NMR spectrum was recorded for  $L_1$ . A characteristic peak for

the tertiary  $\text{C}_{11}$  atom appeared near  $66$  ppm, which further corroborated this proposition.<sup>26,27</sup>

Single crystals of  $L_1$  could not be obtained for X-ray structural analysis; however, the crystal X-ray structures for  $L_1 \cdot [\text{HgCl}_2]$  (**1a**) and  $L_1 \cdot [\text{HgI}_2]$  (**1b**) were obtained and are shown in Figure 1. X-ray-quality single crystals for **1a** and **1b**

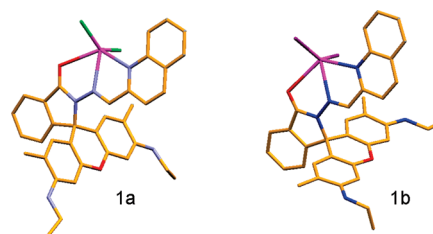


**Figure 1.** Single-crystal X-ray structures for **1a** and **1b**. Hydrogen atoms, lattice chloroform, and methanol molecules are omitted for clarity.

were grown from a  $\text{CHCl}_3/\text{CH}_3\text{OH}$  solution (1:1, v/v) of  $L_1$  and 1.2 mol equiv of  $\text{HgCl}_2$  or  $\text{HgI}_2$  at room temperature by a slow evaporation method.

Mercury diagrams of **1a** and **1b** are depicted in Figure 1, and the structural parameters for both complexes are given in Table 1. Both complexes crystallized in a monoclinic system with space group  $\text{C2}/c$ . In the case of **1a**, two molecules of the metal complex are present in the asymmetric unit along with two  $\text{CHCl}_3$  and one  $\text{CH}_3\text{OH}$  as solvents of crystallization. As depicted in Figure 1, for both compounds, the coordination environment around the central  $\text{Hg}^{\text{II}}$  showed a highly distorted trigonal-bipyramidal geometry in which the triangular base is constituted by the coordinated halide ions and the central azine nitrogen N2 of the rhodamine receptor. The axial positions are occupied by N1 of the quinoline ring and exocyclic ketonic oxygen O1 of the fused bicyclic ring. Interestingly, the second molecule of  $L_1 \cdot [\text{HgCl}_2]$  in the asymmetric unit of **1a** also showed almost identical coordination geometry. Thus, the rhodamine-based receptor acts as a tridentate chelating ligand in the formation of neutral complexes with weak coordination involving the ketonic oxygen O1 with mercury [ $\text{Hg} \cdots \text{O1} = 2.709(4)/2.650(3)$  Å for **1a** and  $\text{Hg} \cdots \text{O1} = 2.809(4)$  Å for **1b**].

The average  $\text{Hg} \cdots \text{Cl}$  distance, considering both molecules present in the asymmetric unit, is  $2.3726(5)$  Å for **1a**, and the  $\text{Hg} \cdots \text{I}$  distance for **1b** is  $2.6435(4)$  Å. The  $\text{Hg} \cdots \text{N}$  distance is in the range  $2.441(4)–2.450(3)$  Å for **1a** and  $2.507(3)–2.566(4)$  Å for **1b**. The crystal lattices are constructed from different types of hydrogen-bonding interactions involving the metal complex and the lattice  $\text{CHCl}_3$  and  $\text{CH}_3\text{OH}$  (via  $\text{N–H} \cdots \text{Cl}$ ,  $\text{O–H} \cdots \text{Cl}$ ,  $\text{N–H} \cdots \text{O}$ , and  $\text{C–H} \cdots \text{O}$  hydrogen bonding) for **1b**,

thus stabilizing the molecule. Thus, *N*-ethyl hydrogen atoms of the rhodamine unit form intermolecular hydrogen bonding with the coordinated Cl1 and Cl3; the OH group of the lattice methanol is involved in O—H...Cl interaction with coordinated Cl3 and the alcoholic oxygen atom acts as an acceptor in N—H...O interaction with the hydrogen atom from the *N*-ethyl group. Hydrogen from both CHCl<sub>3</sub> molecules participates in C—H...O interaction with the exocyclic ketonic oxygen atom of the different metal complexes present in the asymmetric unit holding the volatile solvent molecule in the lattice. No classical hydrogen-bonding interaction is observed for **1b**.

Absorption spectral titrations for **L**<sub>1</sub> ( $7.05 \times 10^{-6}$  M) in an acetonitrile/aqueous HEPES buffer (3:2, v/v) medium with varying pH revealed that the spirocyclic form for **L**<sub>1</sub> was retained for a pH range of 5.0–11.0. Below pH 5.0, a new distinct band appeared at 527 nm, and its intensity was found to increase with a further decrease in the solution pH. This signified the spirolactam ring opening because the acyclic forms of rhodamine 6G derivatives are known to absorb strongly at around 530 nm. As expected, the solution of **L**<sub>1</sub> was found to be nonfluorescent in an acetonitrile/aqueous HEPES buffer (3:2, v/v) solution at neutral pH because of the nonluminescent nature of the spirolactam form of the rhodamine derivative. However, this solution showed a strong fluorescence band with a maximum at 555 nm upon excitation at 500 nm for pH < 3.0. This also corroborated the appreciable spirolactam ring-opening reaction of **L**<sub>1</sub> at pH < 3.0 because the xanthene forms of rhodamine 6G derivatives are known to be strongly fluorescent with an emission maximum at around 560 nm (Figure 2).<sup>28</sup> Thus, the pH range of 5–11 is suitable for using

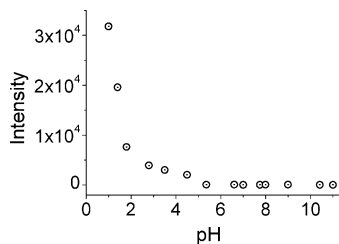


**Figure 2.** Change in the emission intensity at 555 nm with variation in the pH of the acetonitrile/aqueous HEPES buffer (3:2, v/v) solution for **L**<sub>1</sub>.

this reagent as a probe molecule for the detection of any metal ion.

Earlier reports reveal that certain transition-metal ions bind selectively with appropriate derivatives of rhodamine, where metal-ion binding induces opening of the spirolactam ring and generation of the xanthene form with associated changes in the electronic and fluorescence spectral patterns. Thus, we checked the binding affinity of the reagent **L**<sub>1</sub> toward a series of groups 1A (Li<sup>+</sup>, Na<sup>+</sup>, K<sup>+</sup>, and Cs<sup>+</sup>) and 2A (Mg<sup>2+</sup>, Ba<sup>2+</sup>, Ca<sup>2+</sup>, and Sr<sup>2+</sup>) and all common transition-metal ions (Fe<sup>2+</sup>, Fe<sup>3+</sup>, Co<sup>2+</sup>, Ni<sup>2+</sup>, Cu<sup>2+</sup>, Zn<sup>2+</sup>, Cd<sup>2+</sup>, Pb<sup>2+</sup>, Cr<sup>3+</sup>, and Hg<sup>2+</sup>) by monitoring the change in the electronic and fluorescence spectral patterns in a CH<sub>3</sub>CN/aqueous HEPES buffer (3:2, v/v; pH 7.3) medium. Absorption spectra (Figure 3a) revealed a distinct change and the appearance of a new spectral band with a maximum at 527 nm only for Hg<sup>2+</sup> and a maximum at 531 nm for Cr<sup>3+</sup>; the extent of the change in the absorption intensity was more prominent for Hg<sup>2+</sup> (Figure 3). For all of the other ions used for this study, no change in the absorption spectra of **L**<sub>1</sub> was

observed. For Hg<sup>2+</sup> and Cr<sup>3+</sup>, spectral changes were also associated with a visually detectable change from colorless to pink-red, while no such change could be visually detected for any other cations studied. These tend to suggest that the reagent **L**<sub>1</sub> could bind selectively to Hg<sup>2+</sup> and Cr<sup>3+</sup> in a CH<sub>3</sub>CN/HEPES buffer (3:2, v/v) medium of pH 7.3. Interestingly, the use of a comparable concentration of HgX<sub>2</sub> (X<sup>−</sup> = Cl<sup>−</sup> or I<sup>−</sup>) failed to induce any detectable change in the absorption spectra for a predried and distilled acetonitrile solution of the reagent **L**<sub>1</sub>. Spectra for this receptor in the presence of comparable concentrations of Hg(ClO<sub>4</sub>)<sub>2</sub> and HgCl<sub>2</sub> are shown in the inset in Figure 3a. For HgCl<sub>2</sub>, no spectral change was observed when studies were done in a CH<sub>3</sub>CN/HEPES buffer medium (3:2, v/v) of pH 7.3.

The selective binding of **L**<sub>1</sub> to Hg<sup>2+</sup> and Cr<sup>3+</sup> among all other metal ions was also studied using the emission spectral response of the solution of **L**<sub>1</sub> ( $10.0 \times 10^{-6}$  M) in the absence and presence of an excess (14.3 mol equiv) of each of these metal ions in CH<sub>3</sub>CN/aqueous HEPES buffer (3:2, v/v) having a pH of 7.3 (Figure 3b). Among the various metal ions studied, a new strong emission band with a maximum at 555 nm appeared only for Hg<sup>2+</sup> and Cr<sup>3+</sup>. Quantum yield evaluation for **L**<sub>1</sub> was not possible because it shows negligible absorbance at 530 nm in CH<sub>3</sub>CN/aqueous HEPES buffer (3:2, v/v) of pH 7.3; however, the quantum yields ( $\Phi$ ) for **L**<sub>1</sub> in the presence of Hg(ClO<sub>4</sub>)<sub>2</sub> and Cr(ClO<sub>4</sub>)<sub>3</sub> were found to be 0.85 and 0.75, respectively, when the acyclic xanthene form of rhodamine 6G was used as a reference ( $\lambda_{\text{ext}} = 500$  nm). Earlier reports reveal that the spirolactam ring in rhodamine 6G derivatives opens up and converts to the xanthene form upon coordination to a metal ion and the corresponding xanthene derivatives absorb and emit strongly at around 530 and 560 nm, respectively.<sup>29</sup> Thus, the new emission band at 556 nm could be ascribed to the binding of the reagent **L**<sub>1</sub> only to Hg<sup>2+</sup> or Cr<sup>3+</sup> in a CH<sub>3</sub>CN/aqueous HEPES buffer (3:2, v/v) medium of pH 7.3. In general, Hg<sup>2+</sup> is known to quench the emission of a fluorophore because of an efficient spin–orbit coupling.<sup>19c,30</sup> Cr<sup>3+</sup>, being a paramagnetic species, is also expected to cause an emission quenching of a fluorophore.<sup>31</sup> Thus, considering these, the “switch-on” fluorescence response of the reagent **L**<sub>1</sub> upon selective binding to these two ions is of significance. Interestingly, the “switch-on” fluorescence response was observed for Hg<sup>2+</sup> only when Hg<sup>II</sup> salts in the form of Hg(ClO<sub>4</sub>)<sub>2</sub> or Hg(NO<sub>3</sub>)<sub>2</sub> were used.

The relative affinities of Hg<sup>2+</sup> and Cr<sup>3+</sup> (both as perchlorate salts) toward **L**<sub>1</sub> were evaluated from the data of the systematic spectrophotometric titration experiments in a CH<sub>3</sub>CN/aqueous HEPES buffer (pH 7.3; 3:2, v/v) medium (Figure 4). For these, [**L**<sub>1</sub>] was maintained at  $7.05 \times 10^{-6}$  M for studies with Hg(ClO<sub>4</sub>)<sub>2</sub> and [**L**<sub>1</sub>] was maintained at  $7.76 \times 10^{-6}$  M for studies with Cr(ClO<sub>4</sub>)<sub>3</sub>, while [Hg(ClO<sub>4</sub>)<sub>2</sub>] or [Cr(ClO<sub>4</sub>)<sub>3</sub>] was varied between 0 and  $7.14 \times 10^{-4}$  M or between 0 and  $1.02 \times 10^{-3}$  M, respectively (Figure 4). A new band appeared with a gradual increase in the absorbance intensity at 527 nm for Hg(ClO<sub>4</sub>)<sub>2</sub> and at 531 nm for Cr(ClO<sub>4</sub>)<sub>3</sub> (Figure 4). In both instances, a change in the solution color from colorless to pink-red was observed. A B–H plot of  $1/(A - A_0)$  against  $1/[\text{Hg}^{2+}]$  or  $1/(A - A_0)$  against  $1/[\text{Cr}^{3+}]$  was linear. The goodness of linear fit confirms the 1:1 binding stoichiometry between the reagent **L**<sub>1</sub> and Hg<sup>2+</sup> or Cr<sup>3+</sup>, and the respective association constants for **L**<sub>1</sub>·Hg(ClO<sub>4</sub>)<sub>2</sub> and **L**<sub>1</sub>·Cr(ClO<sub>4</sub>)<sub>3</sub> were found to be  $3.11 \times 10^3$  and  $2.0 \times 10^3$  M<sup>−1</sup>, respectively. Spectral response and association constant values remain unchanged

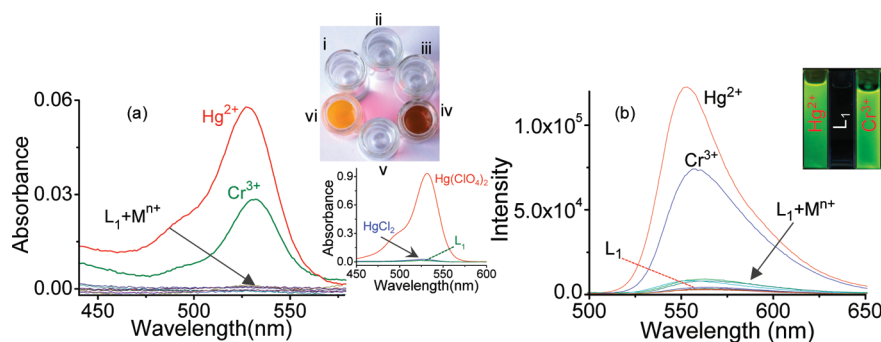


**Figure 3.** Electronic spectra of (a)  $L_1$  ( $7.06 \times 10^{-6}$  M) with different metal ions ( $1.0 \times 10^{-4}$  M) and emission spectra of (b)  $L_1$  ( $10.0 \times 10^{-6}$  M) with different metal ions ( $2.0 \times 10^{-4}$  M) in  $CH_3CN$ /aqueous HEPES buffer (3:2, v/v) of pH 7.3;  $M^{n+} = Li^+$ ,  $Na^+$ ,  $K^+$ ,  $Cs^+$ ,  $Mg^{2+}$ ,  $Ca^{2+}$ ,  $Ba^{2+}$ ,  $Sr^{2+}$ ,  $Cu^{2+}$ ,  $Ni^{2+}$ ,  $Zn^{2+}$ ,  $Cd^{2+}$ ,  $Co^{2+}$ ,  $Fe^{2+}$ ,  $Fe^{3+}$ , and  $Pb^{2+}$ . Inset: Change in the color of  $L_1$  ( $7.06 \times 10^{-6}$  M) in  $CH_3CN$ /aqueous HEPES buffer (3:2, v/v) of pH 7.3 in the absence and presence of different metal ions: (i)  $L_1$ , (ii) in the presence of alkali metal ions ( $Li^+$ ,  $Na^+$ ,  $K^+$ , and  $Cs^+$ ); (iii) in the presence of alkaline-earth metal ions ( $Mg^{2+}$ ,  $Ca^{2+}$ ,  $Ba^{2+}$ , and  $Sr^{2+}$ ); (iv) in the presence of  $Hg^{2+}$  ( $1.0 \times 10^{-4}$  M); (v) in the presence of any one of the transition-metal ions, except  $Cr^{3+}$ ; (vi) in the presence of  $Cr^{3+}$  ( $1.0 \times 10^{-4}$  M). Inset: Electronic spectra of  $L_1$  ( $1.12 \times 10^{-5}$  M) in the presence of  $Hg(ClO_4)_2$  ( $6.25 \times 10^{-4}$  M) and  $HgCl_2$  ( $6.25 \times 10^{-4}$  M) in a  $CH_3CN$  medium. Inset: Change in the observed emission of  $L_1$  ( $7.06 \times 10^{-6}$  M) in  $CH_3CN$ /aqueous HEPES buffer (3:2, v/v) of pH 7.3 in the absence and presence of  $Hg^{2+}$  and  $Cr^{3+}$  ions added as the perchlorate salt.

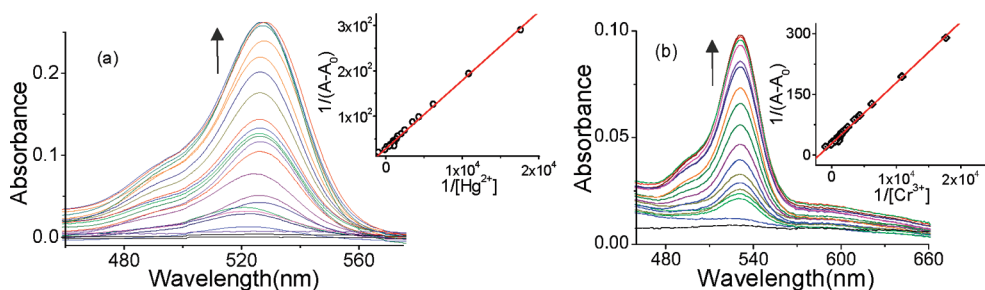


**Figure 4.** Electronic spectra of (a)  $L_1$  ( $7.05 \times 10^{-6}$  M) in the absence and presence of varying  $[Hg(ClO_4)_2]$  ( $0$ – $7.14 \times 10^{-4}$  M) and (b)  $L_1$  ( $7.76 \times 10^{-6}$  M) in the absence and presence of varying  $Cr^{3+}$  ( $0$ – $1.02 \times 10^{-3}$  M) in an acetonitrile/aqueous HEPES buffer (1 mM) (3:2, v/v) solution of pH 7.3. Insets: linear fits of the B–H plots in support of the 1:1 binding stoichiometry for  $L_1 \cdot Hg^{2+}$  and  $L_1 \cdot Cr^{3+}$  formation. The  $ClO_4^-$  salt of both metal ions was used for these studies.

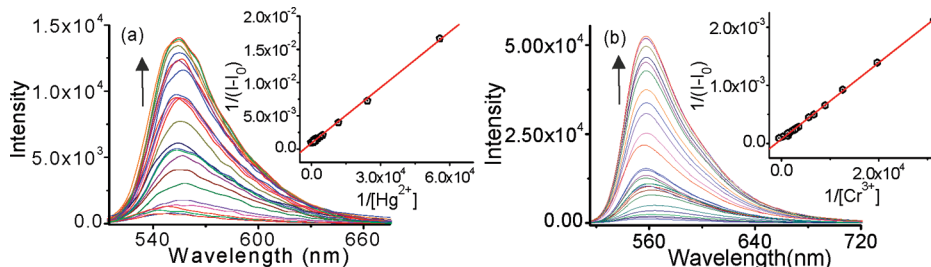


**Figure 5.** Plot of the change in the fluorescence spectral pattern for receptor (a)  $L_1$  ( $7.0 \times 10^{-6}$  M) in the presence of varying  $[Hg(ClO_4)_2]$  ( $0$ – $6.39 \times 10^{-4}$  M) or (b)  $L_1$  ( $7.76 \times 10^{-6}$  M) in the presence of varying  $[Cr(ClO_4)_3]$  ( $0$ – $7.93 \times 10^{-4}$  M) in a  $CH_3CN$ /HEPES buffer medium (1 mM; 3:2, v/v) of pH 7.3;  $\lambda_{ext} = 500$  nm was used for the studies. Insets: Goodness of the linear fits of the B–H plot confirming the 1:1 binding stoichiometry.

when the spectrophotometric titration experiment was repeated using  $Hg(NO_3)_2$ , instead of  $Hg(ClO_4)_2$  in  $CH_3CN$ /aqueous HEPES buffer (3:2, v/v) of pH 7.3. This revealed that counteranions did not have any influence on the binding process with receptor  $L_1$  and the affinity constants for  $Hg^{II}$  salts, which were primarily ionic in nature. The results of the ESI-MS studies further supported a 1:1 binding stoichiometry for the reaction between  $L_1$  and  $Hg(ClO_4)_2$  or  $Cr(ClO_4)_3$  (Supporting Information).

Emission spectra and the intensity at 556 nm remained unchanged for the pH ranges of 5–8.9 for  $Hg^{2+}$  and 5–8.5 for  $Cr^{3+}$  (Supporting Information). Thus, the binding constants for the formation of  $L_1 \cdot Hg(ClO_4)_2$  and  $L_1 \cdot Cr(ClO_4)_3$  in a

$CH_3CN$ /HEPES buffer (3:2, v/v) medium were evaluated at pH 7.3 using systematic emission titration studies (Figure 5). As mentioned earlier, free  $L_1$  did not show any fluorescence upon excitation at 500 nm, and the new emission band at around 556 nm appeared due to formation of the corresponding xanthene form upon coordination to the  $Hg^{2+}$  or  $Cr^{3+}$  ion. The respective binding constants were also evaluated. The formation constants for  $L_1 \cdot Hg(ClO_4)_2$  ( $K_{Hg^{2+}Flu}$ ) and  $L_1 \cdot Cr(ClO_4)_3$  ( $K_{Cr^{3+}Flu}$ ) were found to be  $3.84 \times 10^3$  and  $2.1 \times 10^3$   $M^{-1}$ , respectively, while the lowest detection limit was 10.72 ppm for  $Hg^{2+}$  and 5.6 ppm for  $Cr^{3+}$ . These values were close to those calculated from the absorption titration data. For both cations, namely,  $Hg^{2+}$  and  $Cr^{3+}$ , a 1:1



binding stoichiometry was confirmed from the goodness of the linear fit of the B–H plot (insets in Figure 5), as well as from Job's plot (Supporting Information), using data obtained from either the emission or absorption spectral titration titrations for the respective ions. A higher solvation energy for  $\text{Cr}^{3+}$  ( $H_{\text{hyd}} = 4639 \text{ kJ mol}^{-1}$ ) in water compared to that of  $\text{Hg}^{2+}$  ( $H_{\text{hyd}} = 1824 \text{ kJ mol}^{-1}$ ) could have contributed to a weaker binding of  $\text{Cr}^{3+}$  to the reagent  $\text{L}_1$  than that of  $\text{Hg}^{2+}$ .

As mentioned earlier, the electronic and emission spectral responses were insignificant when either  $\text{HgCl}_2$  or  $\text{HgI}_2$ , instead of  $\text{Hg}(\text{ClO}_4)_2$  or  $\text{Hg}(\text{NO}_3)_2$  were used for studies under identical experimental conditions. For  $\text{HgCl}_2$ , much weaker absorption (inset in Figure 3a) and emission bands with maxima at around 526 and 552 nm, respectively, were observed. This tends to suggest that the interaction between  $\text{Hg}^{\text{II}}$  in  $\text{HgX}_2$  ( $\text{X}^- = \text{Cl}^-$  or  $\text{I}^-$ ) and  $\text{L}_1$  was too weak to be able to induce the ring-opening reaction to the spirolactam form and convert the reagent  $\text{L}_1$  to the corresponding xanthene form. This apparent contradiction was resolved by  $^{13}\text{C}$  NMR spectral studies of  $\text{L}_1$  in the absence and presence of varying  $[\text{Hg}(\text{ClO}_4)_2]$  and  $\text{HgCl}_2$ . For the spirolactam ring form, the signal for the tertiary carbon atom ( $\text{C}_{11}$  in Scheme 1) for free  $\text{L}_1$  appeared at 66 ppm. The intensity of this signal at 66 ppm was found to decrease with an increase in  $[\text{Hg}(\text{ClO}_4)_2]$  with the simultaneous appearance and growth of a new signal at 116 ppm. This signified the opening of the lactam ring with simultaneous xanthene ring formation of  $\text{L}_1$  upon coordination to  $\text{Hg}^{\text{II}}$  of  $\text{Hg}(\text{ClO}_4)_2$ . No such changes were observed when  $^{13}\text{C}$  NMR spectra were recorded in the presence of increasing  $[\text{HgCl}_2]$ , and the signal for the tertiary carbon atom was retained even in the presence of 1.2 mol equiv of  $\text{HgCl}_2$  (Supporting Information). Thus, the results of the  $^{13}\text{C}$  NMR studies also corroborate our results of the absorption and emission spectra, which reveal that  $\text{HgCl}_2$  fails to induce the lactam ring-opening reaction in  $\text{L}_1$  and generation of the xanthene form. Further and more conclusive proof for  $\text{HgCl}_2$  in failing to induce the ring-opening reaction for  $\text{L}_1$  even after coordination to the  $\text{Hg}^{\text{II}}$  center of  $\text{HgX}_2$  was apparent from the single-crystal X-ray structures for  $\text{L}_1 \cdot \text{HgX}_2$  ( $\text{X}^- = \text{Cl}^-$  or  $\text{I}^-$ ; Figure 1).  $\text{HgCl}_2$  possesses only 23% ionic character, and that for  $\text{HgI}_2$  is even less.<sup>22</sup> Presumably, this lower ionic character for  $\text{HgX}_2$  ( $\text{X}^- = \text{Cl}^-$  or  $\text{I}^-$ ) accounts for the lower acidity of the  $\text{Hg}^{\text{II}}$  center and its ability to induce the ring-opening reaction. The binding constant and stoichiometry for  $\text{1a}$  formation were also evaluated based on the small changes that were observed for systematic absorption and emission titration, keeping  $[\text{L}_1]$  ( $1.128 \times 10^{-5} \text{ M}$ ) constant and varying  $[\text{HgCl}_2]$  between 0 and  $1.6 \times 10^{-3} \text{ M}$ . Binding constant values that were evaluated from absorption and emission titration data are 90 and  $125 \text{ M}^{-1}$ , respectively (Supporting Information). In both cases, 1:1 binding stoichiometry was established by the goodness of the linear fit of the B–H plot.

The reversibility of the binding process between  $\text{L}_1$  and  $\text{Hg}^{2+}$  or  $\text{Cr}^{3+}$  was established when the original spectrum for  $\text{L}_1$  was restored upon the addition of either  $\text{I}^-$  as an aqueous solution of KI to the solution of  $\text{L}_1 \cdot \text{Hg}(\text{ClO}_4)_2$  or  $\text{EDTA}^{2-}$  to the solution of  $\text{L}_1 \cdot \text{Cr}(\text{ClO}_4)_3$  in a  $\text{CH}_3\text{CN}$ /aqueous HEPES buffer (3:2, v/v) medium of pH 7.3.  $\text{I}^-$  and  $\text{EDTA}^{2-}$  have a strong affinity for  $\text{Hg}^{2+}$  and  $\text{Cr}^{3+}$ , respectively, and the respective binding constants are much higher than that for  $\text{L}_1$ . This caused demetalation of the reagent  $\text{L}_1$  and regeneration of the spirolactam ring with bleaching of the absorption band at  $\sim 530 \text{ nm}$  and the emission band at around 555 nm. Thus,

reagent  $\text{L}_1$  could be used as a reversible sensor for the recognition of  $\text{Hg}^{2+}$  and  $\text{Cr}^{3+}$  in a mixed-solvent medium under physiological conditions (Supporting Information). The reversibility in the binding of  $\text{L}_1$  to  $\text{Hg}^{2+}$  in the presence of an excess of KI could be further extended for use of the reagent  $\text{L}_1$  as a selective chemosensor for  $\text{Cr}^{3+}$ . In the presence of an excess of KI,  $\text{HgI}_2$  was formed preferentially, and this caused restoration of the original spectra for  $\text{L}_1$  with formation of the cyclic lactam form of the reagent (*vide infra*)  $\text{L}_1$ . Again, upon the addition of  $\text{Cr}^{3+}$  to this solution mixture having KI, the absorbance band at 530 nm and the emission band at 557 nm reappeared (Supporting Information) and the pink color of the solution was also restored. Preferential binding of the iodide ion to the  $\text{Hg}^{2+}$  ion led to the formation of  $\text{HgI}_2$  and the cyclic lactam form of the reagent  $\text{L}_1$ . However, the absorption and emission spectral bands, as well as the solution color for the acyclic xanthene form of the reagent, were restored upon coordination of the  $\text{Cr}^{3+}$  ion to  $\text{L}_1$ . Further experiments revealed that the absorbance spectra for  $\text{L}_1 \cdot \text{Cr}^{3+}$  and its solution color remained unchanged upon the addition of an excess of the iodide ion in the form of KI. Thus, in the presence of an excess of KI, reagent  $\text{L}_1$  could also be used for the selective recognition of  $\text{Cr}^{3+}$  from all other metal ions.

Weaker binding of  $\text{L}_1$  to the  $\text{Hg}^{2+}$  center in  $\text{1a}$  compared to that in  $\text{L}_1 \cdot \text{Hg}(\text{ClO}_4)_2$  was also evident from the FTIR spectra recorded for  $\text{L}_1$  in the presence of 5 mol equiv of  $\text{HgCl}_2$  and  $\text{Hg}(\text{ClO}_4)_2$ . The stretching frequency for the  $\text{C}=\text{O}$  bond for  $\text{L}_1$  appeared at  $1695 \text{ cm}^{-1}$ , while it appeared at  $1684 \text{ cm}^{-1}$  in the presence of  $\text{HgCl}_2$  and at  $1647 \text{ cm}^{-1}$  in the presence of  $\text{Hg}(\text{ClO}_4)_2$  (Supporting Information). A larger shift signifies a higher polarization of the  $\text{C}=\text{O}$  bond upon more efficient binding to the  $\text{Hg}^{2+}$  center in  $\text{Hg}(\text{ClO}_4)_2$ .

The influence of the binding of  $\text{Hg}^{2+}$  or  $\text{Cr}^{3+}$  to the receptor  $\text{L}_1$  on the lifetime of its excited state was further checked from the results of the TCSPC studies using a 360 nm nano-LED as the excitation source. Emission decay traces ( $\lambda_{\text{Mon}} = 550 \text{ nm}$ ) for receptor  $\text{L}_1$  ( $7.76 \times 10^{-6} \text{ M}$ ) could be best fitted with a biexponential function with time constants  $\tau_1 = 0.19 \pm 0.01$  (37.08%) and  $\tau_2 = 2.80 \pm 0.07$  (62.09%) with  $\chi^2 = 1.241 \text{ ns}$ , whereas the same receptor showed a biexponential decay with the time constants  $\tau_1 = 0.02 \pm 0.05$  (12.41%) and  $\tau_2 = 2.8 \pm 0.05$  (87.59%) having  $\chi^2 = 1.02 \text{ ns}$  in the presence of the  $\text{Hg}^{2+}$  ion, added as  $\text{Hg}(\text{ClO}_4)_2$ . The minor and short-lived component was assigned to the decay time for the excited state related to the spirolactam moiety, while the long-lived major component was attributed to the xanthene form of the reagent  $\text{L}_1$ .<sup>19b</sup> The relative increase in the percentage of the open-ring xanthene form upon the addition of  $\text{Hg}^{2+}$  confirms the interaction of  $\text{Hg}^{2+}$  with the receptor. A similar experiment performed with comparable  $[\text{Cr}(\text{ClO}_4)_3]$  showed a biexponential decay trace with time constants  $\tau_1 = 0.97 \pm 0.03$  (44%) and  $\tau_2 = 4.13 \pm 0.12$  (56%).

A comparison of the absorption spectra for free reagent  $\text{L}$  and  $\text{L}_1$  revealed additional absorption bands at 332 and 347 nm for  $\text{L}_1$ . Analogous quinoline derivatives are known to have an absorption band within the range 310–350 nm. Thus, an exact assignment of the absorption band for the quinoline fragment in  $\text{L}_1$  is difficult. However, one of these two bands at 332 and 347 nm originates from the quinoline fragment and neither free  $\text{L}_1$  nor  $\text{L}_1 \cdot \text{Hg}(\text{ClO}_4)_2$  or  $\text{L}_1 \cdot \text{Cr}(\text{ClO}_4)_3$  showed any characteristic emission band for the quinoline fragment even upon excitation at  $\sim 332$  or  $\sim 347 \text{ nm}$ , where the quinoline fragment is expected to absorb (Supporting Information).<sup>16a,32</sup> Let us address this



apparently anomalous observation. In the case of  $L_1$ , the flexibility and rapid  $C=N$  isomerization of the imine functionality coupled to the quinoline fragment could be responsible for the nonradiative deactivation of the quinoline-based excited state and quenching of the quinoline-based emission for  $L_1$ .<sup>19c,33</sup> Further, literature reports reveal that the ring nitrogen atom of the quinoline moiety is strongly hydrogen-bonded with water molecules in aqueous or mixed aqueous medium and forms a stoichiometric complex between the excited state of quinoline and a solvent molecule (exciplex),<sup>19c,34</sup> which could also have contributed to the observed quenching of the quinoline-based emission. For  $L_1 \cdot Hg(ClO_4)_2$  and  $L_1 \cdot Cr(ClO_4)_3$ , it may be presumed that the efficient spin-orbit coupling for  $Hg^{2+}$  and the strong paramagnetic influence of the  $Cr^{3+}$  ion could be responsible for quenching of the quinoline-based emission.

**Cell Imaging Study.**  $Hg^{2+}$  is known to exert an estrogenic effect on breast cancer cells by binding to estrogen receptors and causing increased cell growth. Among heavy metal ions, chromium is found to be in higher amounts in human breast cancer tumor samples than in benign breast tissue.<sup>35</sup> These reports relate these metal ions to malignancy and led us to check the possibility of using the reagent  $L_1$  as an imaging agent for the detection of these toxic metal ions in human breast cancer cells.

The  $L_1$ -stained breast cancer cell MCF7 treated with either  $Cr^{3+}$  or  $Hg^{2+}$  was visualized under the laser scanning confocal microscope FV1000 (Olympus), as mentioned in the Materials and Methods section. MCF7 cells treated with different concentrations of  $Cr^{3+}$  (Figure 6A) or  $Hg^{2+}$  (Figure 6B)

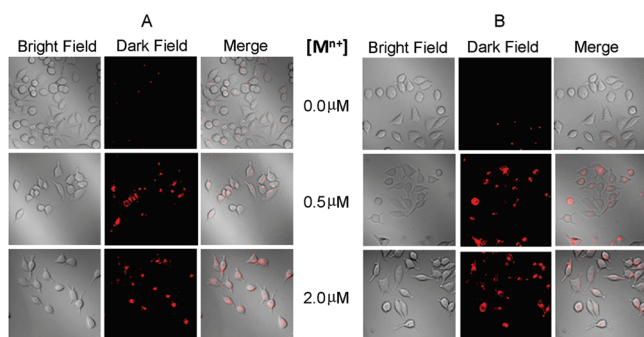


**Figure 6.** Confocal images of (A)  $Cr^{3+}$ - and (B)  $Hg^{2+}$ -treated MCF7 cells. The cells were supplemented with different concentrations of  $Cr(ClO_4)_3$  or  $Hg(ClO_4)_2$  (0.0  $\mu M$ ; A, 0.5  $\mu M$ ; B, 2.0  $\mu M$ ) in the growth media for 1.0 h at 37  $^{\circ}C$  followed by staining with 4.0  $\mu M$   $L_1$  for 1.0 h at 37  $^{\circ}C$  ( $\lambda_{ext} = 543$  nm).

showed brighter fluorescence in comparison to untreated cells with no or very little fluorescence. The fluorescence was mostly localized in the cytoplasm of the cells. The results also indicate that  $L_1$  could detect  $Cr^{3+}$  or  $Hg^{2+}$  at the 0.5  $\mu M$  level. The reversibility of the binding of the reagent  $L_1$  to  $Hg^{2+}$  or  $Cr^{3+}$  ions present in MCF7 cells could also be established by recording confocal images of the stained cells in the presence of an excess (5 mol equiv with respect to  $L_1$ ) of KI [for  $Hg(ClO_4)_2$ ] or  $Na_2EDTA$  [for  $Cr(ClO_4)_3$ ]; a substantial decrease in fluorescence of the MCF7 cells, previously treated with the respective metal ions and the reagent  $L_1$ , upon exposure to iodide or  $EDTA^{2-}$  ions was observed (Supporting Information).

Further, the cytotoxicity of  $L_1$  on MCF7 cells was determined by a conventional MTT assay (Supporting Information),<sup>36</sup> which revealed that, upon exposure to a 5  $\mu M$  concentration of  $L_1$  (a concentration that was comparable to that used for confocal imaging studies; Figure 6) for 6 h,  $\sim 87\%$  of the MCF7 cells remained viable. This nullified the possibility of any significant cytotoxic influence of the reagent  $L_1$  on MCF7 cells. Therefore, it may be concluded that  $L_1$  could be used as a viable chemosensor for  $Cr^{3+}$  or  $Hg^{2+}$  in biological samples.

In brief, we have reported a new rhodamine-based reagent ( $L_1$ ) that showed remarkable preference toward  $Hg^{2+}$  and  $Cr^{3+}$ . Upon binding to either of these two ions, a visually detectable change in the color and emission were observed because of conversion of the lactam form of the rhodamine derivative to the acyclic xanthene form. This offered the possibility of using this reagent for use either as a colorimetric or as a fluorescence-based reagent for the detection of larger fluctuations of these ions, especially in the case of  $Hg^{2+}$ , which binds at a micromolar level under physiological conditions. Further studies revealed that conversion from the cyclic lactam form to the acyclic xanthene form was reversible, and thus this reagent could be used as a reversible sensor for the detection of  $Hg^{2+}$  or  $Cr^{3+}$ . More importantly, reagent  $L_1$  could be used as an imaging agent for detection of these ions, which are known for their deleterious influence in cell malignancy, in breast cancer cell MCF7. More importantly, this is the first report on the single-crystal structure for  $HgX_2$  ( $X = Cl$  or  $I$ ) bound to a lactam form of the rhodamine derivative and explicitly explains the inability of these lactam reagents to recognize mercury halides through detectable changes in optical or fluorescence spectra.

## ■ ASSOCIATED CONTENT

### ● Supporting Information

Characterization data of the receptor  $L_1$ , spectral crystallographic details, biological studies, and X-ray crystallographic data in CIF format. This material is available free of charge via the Internet at <http://pubs.acs.org>.

## ■ AUTHOR INFORMATION

### Corresponding Author

\*E-mail: [sudip@hijli.iitkgp.ernet.in](mailto:sudip@hijli.iitkgp.ernet.in) (S.K.G.), [amitava@csmcni.org](mailto:amitava@csmcni.org) (A.D.). Tel: +91 278 2567760 [672]. Fax: +91 278 2656762.

## ■ ACKNOWLEDGMENTS

A.D. acknowledges DST and CSIR for financial support. S.S., P.M., and A.C. acknowledge CSIR, while U.R.G. and M.B. acknowledge UGC for their fellowships. S.K.G. acknowledges FIST and DST for Confocal facilities at IIT, Kharagpur, India. A.D. thanks Dr. P. K. Ghosh (Director), CSMCRI, Bhavnagar, India, for his keen interest in this work.

## ■ REFERENCES

- (1) (a) Chen, T.; Zhu, W.; Xu, Y.; Zhang, S.; Zhang, X.; Qian, X. *Dalton Trans.* **2010**, 39, 1316–1320. (b) Ho, M.-L.; Chen, K.-Y.; Lee, G.-H.; Chen, Y.-C.; Wang, C.-C.; Lee, J.-F. *Inorg. Chem.* **2009**, 48, 10304–10311. (c) Huang, W.; Zhou, P.; Yan, W.; He, C.; Xiong, L.; Li, F.; Duan, C. *J. Environ. Monit.* **2009**, 11, 330–335.
- (2) (a) Zhao, Y.; Sun, Y.; Lv, X.; Liu, Y.; Chen, M.; Guo, W. *Org. Biomol. Chem.* **2010**, 8, 4143–4147. (b) Samb, I.; Bell, J.; Toullec, P. Y.; Michelet, V.; Leray, I. *Org. Lett.* **2011**, 13, 1182–1185. (c) Xie, Z.; Wang, K.; Zhang, C.; Yang, Z.; Chen, Y.; Guo, Z.; Lua, G.-Y.; He, W.

- New J. Chem.* **2011**, 35, 607–613. (d) Huang, J.; Xu, Y.; Qian, X. *J. Org. Chem.* **2009**, 74, 2167–2170.
- (3) (a) Pires, M. M.; Chmielewski, J. *Org. Lett.* **2008**, 10, 837–840. (b) Balendiran, G. K.; Dabur, R.; Fraser, D. *Cell Biochem. Funct.* **2004**, 22, 343–352.
- (4) (a) Clarkson, T. W.; Magos, L.; Myers, G. J. *N. Engl. J. Med.* **2003**, 18, 1731–1737. (b) Mahato, P.; Ghosh, A.; Saha, S.; Mishra, S.; Mishra, S. K.; Das, A. *Inorg. Chem.* **2010**, 49, 11485–11492. (c) Wanga, Q.; Kima, D.; Dionysiou, D. D.; Soriala, G. A.; Timberlake, D. *Environ. Pollut.* **2004**, 131, 323–336. (d) Harris, H. H.; Pickering, I. J.; George, G. N. *Science* **2003**, 301, 1203.
- (5) (a) Li, C.; Liu, S. *J. Mater. Chem.* **2010**, 20, 10716–10723. (b) Misra, A.; Shahid, M. *J. Phys. Chem. C* **2010**, 114, 16726–16739. (c) Zhou, Y.; You, X.-Y.; Fang, Y.; Li, J.-Y.; Liu, K.; Yao, C. *Org. Biomol. Chem.* **2010**, 8, 4819–4822. (d) Nolan, E. M.; Lippard, S. J. *J. Am. Chem. Soc.* **2003**, 125, 14270–14271.
- (6) (a) Nolan, E. M.; Lippard, S. J. *Chem. Rev.* **2008**, 108, 3443–3480. (b) Mason, R. P.; Morel, F. M. M.; Hemond, H. F. *Water, Air, Soil Pollut.* **1995**, 80, 775.
- (7) (a) Huang, K.; Yang, H.; Zhou, Z.; Yu, M.; Li, F.; Gao, X.; Yi, T.; Huang, C. *Org. Lett.* **2008**, 10, 2557–2560. (b) Latva, S.; Jokiniemi, J.; Peraniemi, S.; Ahlgren, M. *J. Anal. At. Spectrom.* **2003**, 18, 84–85. (c) Singh, A. K.; Gupta, V. K.; Gupta, B. *Anal. Chim. Acta* **2007**, 585, 171–178. (d) Zayed, A. M.; Terry, N. *Plant Soil* **2003**, 249, 139–156.
- (8) (a) Zhou, Z.; Yu, M.; Yang, H.; Huang, K.; Li, F.; Yi, T.; Huang, C. *Chem. Commun.* **2008**, 3387–3389. (b) Vincent, J. B. *Nutr. Rev.* **2000**, 58, 67–72.
- (9) Latmani, R. B.; Obratsova, A.; Mackey, M. R.; Ellisman, M. H.; Tebo, B. M. *Environ. Sci. Technol.* **2007**, 41, 214–220.
- (10) (a) Snow, E. T. *Environ. Health Perspect.* **1994**, 102, 41–44. (b) Klein, C. B.; Frenkel, K.; Costa, M. *Chem. Res. Toxicol.* **1991**, 4, 592–604. (c) De Flora, S.; Bagnasco, M.; Serra, D.; Zanacchi, P. *Mutat. Res.* **1990**, 238, 99–172.
- (11) (a) Mandal, A. K.; Suresh, M.; Mishra, S. K.; Mishra, S.; Das, A. *Sens. Actuators, B* **2010**, 145, 32–38. (b) Suresh, M.; Mishra, S. K.; Mishra, S.; Das, A. *Chem. Commun.* **2009**, 2496–2498.
- (12) (a) Culp, J. H.; Windham, R. L.; Wheal, R. D. *Anal. Chem.* **1971**, 43, 1321. (b) Beauchemin, D. *Anal. Chem.* **2008**, 80, 4455–4486.
- (13) (a) Yang, H.; Zhou, Z.; Huang, K.; Yu, M.; Li, F.; Yi, T.; Huang, C. *Org. Lett.* **2007**, 9, 4729–4732. (b) Gong, J.; Zhou, T.; Song, D.; Zhang, L.; Hu, H. *Anal. Chem.* **2010**, 82, 567–573. (c) Alfonso, M.; Tarraga, A.; Molina, P. *Dalton Trans.* **2010**, 8637–8645. (d) Zhao, Q.; Cao, T.; Li, X.; Jing, H.; Yi, T.; Huang, C. *Organometallics* **2007**, 26, 2077–2081.
- (14) (a) Chen, C.; Wang, R.; Guo, L.; Fu, N.; Dong, H.; Yuan, Y. *Org. Lett.* **2011**, 13, 1162–1165. (b) Hu, J.; Dai, L.; Liu, S. *Macromolecules* **2011**, 44, 4699–4710. (c) Caballero, A.; Martínez, R.; Lloveras, V.; Ratera, I.; Vidal-Gancedo, J.; Würst, K.; Tarraga, A.; Molina, P.; Veciana, J. *J. Am. Chem. Soc.* **2005**, 127, 15666–15667. (d) Li, T.; Li, B.; Wang, E.; Dong, S. *Chem. Commun.* **2009**, 3551–3553. (e) Zhang, D.; Deng, M.; Xu, L.; Zhou, Y.; Yuwen, J.; Zhou, X. *Chem.—Eur. J.* **2009**, 15, 8117–8120. (f) Loe-Mie, F.; Marchand, G.; Berthier, J.; Sarrut, N.; Pucheault, M.; Blanchard-Desce, M.; Vinet, F.; Vaultier, M. *Angew. Chem., Int. Ed.* **2010**, 49, 422–425. (g) Hu, J.; Zhang, M.; Yu, L. B.; Ju, Y. *Bioorg. Med. Chem. Lett.* **2010**, 20, 4342–4345. (h) Kim, E.; Kim, H. E.; Lee, S. J.; Lee, S. S.; Seo, M. L.; Jung, J. H. *Chem. Commun.* **2008**, 3921–3923. (i) Zhu, M.; Yuan, M.; Liu, X.; Xu, J.; Lv, J.; Huang, C.; Liu, H.; Li, Y.; Wang, S.; Zhu, D. *Org. Lett.* **2008**, 10, 1481–1484. (j) Wu, D.; Descalzo, A. B.; Weik, F.; Emmerling, F.; Shen, Z.; You, X.-Z.; Rurack, K. *Angew. Chem., Int. Ed.* **2008**, 47, 193–197.
- (15) (a) Avirah, R. R.; Jyothish, K.; Ramaiah, D. *Org. Lett.* **2007**, 9, 121–124. (b) Santra, M.; Roy, B.; Ahn, K. H. *Org. Lett.* **2011**, 13, 3422–3425. (c) Ando, S.; Koide, K. *J. Am. Chem. Soc.* **2011**, 133, 2556–2566. (d) Kim, J. H.; Kim, H. J.; Kim, S. H.; Lee, J. H.; Do, J. H.; Kim, H. J.; Lee, J. H.; Kim, J. S. *Tetrahedron Lett.* **2009**, 50, 5958–5961. (e) Chen, X.; Nam, S.-W.; Jou, M. J.; Kim, Y.; Kim, S.-J.; Park, S.; Yoon, J. *Org. Lett.* **2008**, 10, 5235–5238. (f) Che, Y.; Yang, X.; Zang, L. *Chem. Commun.* **2008**, 1413–1415. (g) Dave, N.; Chan, M. Y.; Huang, P.-J. J.; Smith, B. D.; Liu, J. *J. Am. Chem. Soc.* **2010**, 132, 2668–2669. (h) Lee, M. H.; Lee, S. W.; Kim, S. H.; Kang, C.; Kim, J. S. *Org. Lett.* **2009**, 11, 2101–2104. (i) Chen, X.; Baek, K.-H.; Kim, Y.; Kim, S.-J.; Shin, I.; Yoon, J. *Tetrahedron* **2010**, 66, 4016–4021. (j) Kim, H. N.; Nam, S.-W.; Swamy, K. M. K.; Jin, Y.; Chen, X.; Kim, Y.; Kim, S.-J.; Park, S.; Yoon, J. *Analyst* **2011**, 136, 1339–1343. (k) Ahamed, B. N.; Arunachalam, M.; Ghosh, P. *Inorg. Chem.* **2010**, 49, 4447–4457.
- (16) (a) *Principles of Fluorescence Spectroscopy*; Lokowize, J. R., 3rd ed.; Springer: Berlin, 2006. (b) Valeur, B. *Molecular Fluorescence*, 2nd ed.; Wiley-VCH: New York, 2005.
- (17) (a) Kim, H. N.; Lee, M. H.; Kim, H. J.; Kim, J. S.; Yoon, J. *Chem. Soc. Rev.* **2008**, 37, 1465–1472. (b) Beija, M.; Afonso, C. A. M.; Martinho, J. M. G. *Chem. Soc. Rev.* **2009**, 38, 2410–2433. (c) Quang, T. D.; Kim, J. S. *Chem. Rev.* **2010**, 110, 6280–6301. (d) Ahamed, B. N.; Ghosh, P. *Inorg. Chim. Acta* **2011**, 372, 100–107.
- (18) (a) Weerasinghe, A. J.; Schmiesing, C.; Sinn, E. *Tetrahedron Lett.* **2009**, 50, 6407–6410. (b) Mao, J.; Wang, L.; Dou, W.; Tang, X.; Yan, Y.; Liu, W. *Org. Lett.* **2007**, 9, 4567–4570. (c) Wan, Y.; Guo, Q.; Wang, X.; Xia, A. *Anal. Chim. Acta* **2010**, 665, 215–220. (d) Weerasinghe, A. J.; Schmiesing, C.; Sinn, E. *Tetrahedron Lett.* **2009**, 50, 6407–6410.
- (19) (a) Huang, K.; Yang, H.; Zhou, Z.; Yu, M.; Li, F.; Gao, X.; Yi, T.; Huang, C. *Org. Lett.* **2008**, 10, 2557–2560. (b) Suresh, M.; Mishra, S.; Mishra, S. K.; Suresh, E.; Mandal, A. K.; Shrivastav, A.; Das, A. *Org. Lett.* **2009**, 11, 2740–2743. (c) Suresh, M.; Mandal, A. K.; Saha, S.; Suresh, E.; Mandoli, A.; Liddo, R. D.; Parnigotto, P. P.; Das, A. *Org. Lett.* **2010**, 12, 5406–5409. (d) Kumar, M.; Kumar, N.; Bhalla, V.; Singh, H.; Sharma, P. R.; Kaur, T. *Org. Lett.* **2011**, 13, 1422–1425. (e) Chen, X.; Nam, S.-W.; Jou, M. J.; Kim, Y.; Kim, S.-J.; Park, S.; Yoon, J. *Org. Lett.* **2008**, 10, 5235–5238.
- (20) (a) Zhang, X.; Xiao, Y.; Qian, X. *Angew. Chem., Int. Ed.* **2008**, 47, 8025–8029. (b) Ko, S.-K.; Yang, Y.-K.; Tae, J.; Shin, I. *J. Am. Chem. Soc.* **2006**, 128, 14150–14155.
- (21) (a) Shi, W.; Ma, H. *Chem. Commun.* **2008**, 1856–1858. (b) Zhan, X.-Q.; Qian, Z.-H.; Zheng, H.; Su, B.-Y.; Lan, Z.; Xu, J.-G. *Chem. Commun.* **2008**, 1859–1861.
- (22) Clarke, J. H. R.; Solomons, C. *J. Chem. Phys.* **1968**, 48, 528–529.
- (23) (a) Wu, D.; Huang, W.; Duan, C.; He, C.; Wu, S.; Wang, D. *Inorg. Chem.* **2008**, 47, 7190–7201. (b) Dujols, V.; Ford, F.; Czarnik, A. W. *J. Am. Chem. Soc.* **1997**, 119, 7386–7387.
- (24) (a) Sheldrick, G. M. *SHELXL-97: Program for Crystal Structure Refinement*; University of Göttingen: Göttingen, Germany, 1997. (b) SADABS, *Empirical Absorption Correction Program*; University of Göttingen: Göttingen, Germany, 1997. (c) Sheldrick, G. M. *SHELXTL Reference Manual*, version 5.1; Bruker AXS: Madison, WI, 1997. (d) Sheldrick, G. M. *SAINT*, 5.1 ed.; Siemens Industrial Automation Inc.: Madison, WI, 1995.
- (25) (a) Benesi, H. A.; Hildebrand, J. H. *J. Am. Chem. Soc.* **1949**, 71, 2703–2707. (b) Yang, C.; Liu, Y.; Mu, T.-W.; Guo, Q.-X. *Anal. Sci.* **2000**, 16, 537–539. (c) Shiraishi, Y.; Sumiya, S.; Kohno, Y.; Hirai, T. *J. Org. Chem.* **2008**, 73, 8571–8574.
- (26) (a) Wu, D.; Wei, H.; Duan, C.; Lin, Z.; Meng, G. *Inorg. Chem.* **2007**, 46, 1538. (b) Jun, M. E.; Roy, B.; Ahn, K. H. *Chem. Commun.* **2011**, 47, 7583–7601. (c) Beija, M.; Afonso, C. A. M.; Martinho, J. M. G. *Chem. Soc. Rev.* **2009**, 38, 2410–2433.
- (27) (a) Kwon, J. Y.; Jang, Y. J.; Lee, Y. J.; Kim, K.-M.; Seo, M.-S.; Nam, W.; Yoon, J. *J. Am. Chem. Soc.* **2005**, 127, 10107–10108. (b) Anthoni, U.; Christophersen, C.; Nielsen, P.; Puschl, A.; Schaumburg, K. *Struct. Chem.* **1995**, 3, 161.
- (28) (a) Zhang, J. F.; Zhou, Y.; Yoon, J.; Kim, Y.; Kim, S. J.; Kim, J. S. *Org. Lett.* **2010**, 12, 3852–3855. (b) Lin, W.; Cao, X.; Ding, Y.; Yuan, L.; Yu, Q. *Org. Biomol. Chem.* **2010**, 8, 3618–3620. (c) Yang, Y.-K.; Shim, S.; Tae, J. *Chem. Commun.* **2010**, 46, 7766–7768. (d) Suresh, M.; Shrivastav, A.; Mishra, S.; Suresh, E.; Das, A. *Org. Lett.* **2008**, 10, 3013–3016.
- (29) (a) Kim, H. N.; Lee, M. H.; Kim, H. J.; Kim, J. S.; Yoon, J. *Chem. Soc. Rev.* **2008**, 37, 1465–1472. (b) Quang, D. T.; Kim, J. S. *Chem. Rev.* **2010**, 110, 6280–6301.

- (30) (a) McClure, D. S. *J. Chem. Phys.* **1952**, *20*, 682–686.  
(b) Masuhara, H.; Shioyama, H.; Saito, T.; Hamada, K.; Yasoshima, S.; Mataga, N. *J. Phys. Chem.* **1984**, *88*, 5868–5873.
- (31) (a) Rurack, K. *Spectrochim. Acta, Part A* **2001**, *57*, 2161.  
(b) Kim, J. S.; Quang, D. T. *Chem. Rev.* **2007**, *107*, 3780–3799.  
(c) Bergonzi, R.; Fabbrizzi, L.; Licchelli, M.; Mangano, C. *Coord. Chem. Rev.* **1998**, *170*, 31–46.
- (32) Fletcher, A. N. *J. Phys. Chem.* **1968**, *72*, 2742.
- (33) Naik, L. R.; Kumar, S. H. M.; Inamdar, S. R.; Math, N. N. *Spectrosc. Lett.* **2005**, *38*, 645.
- (34) Schulman, S. G.; Capomacchia, A. C. *Anal. Chim. Acta* **1972**, *58*, 91–99.
- (35) (a) Martin, M. B.; Reiter, R.; Pham, T.; Avellanet, Y. R.; Camara, J.; Lahm, M.; Pentecost, E.; Pratap, K.; Gilmore, B. A.; Divekar, S.; Dagata, R. S.; Bull, J. L.; Stoica, A. *Endocrinology* **2003**, *144*, 2425. (b) Sukocheva, O. A.; Yang, Y.; Gierthy, J. F.; Seegal, R. F. *Environ. Toxicol.* **2005**, *20*, 32. (c) Ionescu, J. G.; Novotny, J.; Stejskal, V.; Lätsch, A.; Blaurock-Busch, E.; Eisenmann-Klein, M. *Neuroendocrinol. Lett.* **2006**, *27*, 36–39.
- (36) Rubinstein, L. V.; Paull, K. D.; Simon, R. M.; Skehan, P.; Scudiero, D. A.; Monks, A.; Boyd, M. R. *J. Natl. Cancer Inst.* **1990**, *82*, 1113–1117.